

Spin and Conductance-Peak-Spacing Distributions in Large Quantum Dots: A Density-Functional Theory Study

Hong Jiang,^{1,2,3} Harold U. Baranger,² and Weitao Yang¹

¹*Department of Chemistry, Duke University, Durham, North Carolina 27708-0354*

²*Department of Physics, Duke University, Durham, North Carolina 27708-0305*

³*College of Chemistry and Molecular Engineering, Peking University, Beijing, China 100871*

(Received 7 August 2002; published 17 January 2003)

We use spin-density-functional theory to study the spacing between conductance peaks and the ground-state spin of 2D model quantum dots with up to 200 electrons. Distributions for different ranges of electron number are obtained in both symmetric and asymmetric potentials. The even/odd effect is pronounced for small symmetric dots but vanishes for large asymmetric ones, suggesting substantially stronger interaction effects than expected. The fraction of high-spin ground states is remarkably large.

DOI: 10.1103/PhysRevLett.90.026806

PACS numbers: 73.23.Hk, 73.40.Gk, 73.63.Kv

The interplay of quantum mechanical interference and electron-electron interactions is a current theme in many areas of solid-state physics. A semiconductor quantum dot (QD) [1,2]—a nanodevice in which electron motion is quantized in all three dimensions—is a particularly simple system in which to study this interplay. In Coulomb blockade experiments in the electron tunneling regime, the conductance through the dot varies strongly as a function of gate voltage, forming a series of sharp peaks. For closed dots at low temperature, both the positions and heights of the peaks encode information about the dot's ground state. In particular, the spacing between adjacent conductance peaks is proportional to the second difference of the ground-state energy with respect to electron number N , $\Delta_2 E(N) \equiv E_{gs}(N+1) + E_{gs}(N-1) - 2E_{gs}(N)$, which is often called the addition energy. Furthermore, the ground-state spin of the QD can be inferred from the shift in position of the conductance peaks upon applying a magnetic field.

The addition energy varies because of changing interference conditions either as N changes or from dot to dot, leading to a conductance-peak-spacing distribution. Previous theoretical work addressing this distribution can be divided into roughly two types: First, computational approaches addressed small dots with random disorder—both exact diagonalization [3,4] and self-consistent field methods (Hartree-Fock [5–9] or density-functional theory [10,11]). Second, a semianalytic treatment of large dots was developed based on general statistical assumptions [2,12–16] for irregular quantum dots, which combines a random matrix theory (RMT) [2,17] description of the single-particle energy and a random-phase approximation (RPA) treatment of the screened electron-electron interaction.

The results of these two approaches are quite different. First, for the zero temperature peak spacing, the small dot calculations yield Gaussian-like distributions while the large N results are non-Gaussian. Second, spin degeneracy causes a significant “even/odd effect” in the large dot

approach: the distribution for N even is very different from that for N odd. Third, with regard to the ground-state spin [11,18–21], the small N calculations find an enhancement of the low-spin states compared to the large QD approach.

Experimental work to date [3,22–25] has unfortunately failed to probe the ground-state addition energy distribution or ground-state spin of generic systems. In the more recent experiments, either temperature obscured the ground-state properties [14,15,23,25] or the dot was regular in shape [24].

Our aim here is to bridge the gap between the two theoretical approaches and so highlight the need for experiments. We have used Kohn-Sham (KS) spin density-functional theory (SDFT) [26] to study both the peak spacing and the spin distribution for 2D model QDs. For the exchange-correlation energy, we use Tanatar and Ceperley's 2D parametrization of 2D local spin density approximation (LSDA) [27]. Comparisons with quantum Monte Carlo calculations for $N \leq 8$ and interaction strength parameter $r_s \leq 8$ have shown that LSDA works well for both the ground-state spin and energy in 2D clean parabolic QD [28,29]. Here we obtain statistics with N up to 200 [30]. This is the first calculation, as far as we know, for large realistic QDs.

Our primary result is that the effective electron-electron interaction that emerges is substantially stronger than that predicted from the RPA-RMT treatment. The evidence is twofold: (i) the addition energy distribution is Gaussian-like with no discernible even/odd effect, and (ii) the probability of having a high-spin state ($S \geq 1$) is larger than the maximum possible from RPA-RMT.

We use a quartic potential to model 2D QD systems,

$$V_{\text{ext}}(\mathbf{r}) = a \left[\frac{x^4}{b} + by^4 - 2\lambda x^2 y^2 + \gamma(x^2 y - xy^2)r \right]. \quad (1)$$

Both the classical dynamics and the single-particle quantum mechanics at $\gamma = 0$ have been studied in detail [31]:

the system evolves from integrable to fully chaotic as λ changes from 0 to 1. The parameter γ breaks the fourfold symmetry. The prefactor is $a = 10^{-4}$; this allows the electrons to spread so that the interaction strength parameter, r_s , is about 1.5, close to experimental conditions.

For a given V_{ext} , the ground state energy E_{gs} and spin S_{gs} as a function of N are determined by calculating several spin configurations for each N and selecting the one with minimum energy. The addition energy is then the second difference of $E_{\text{gs}}(N)$ [see Fig. 1(a)]. To obtain good statistics, in both the symmetric and asymmetric cases we calculate five sets of data with different parameters [32]. Correlation analysis shows that the single-particle level spacing (SPLS) and addition energy from the different sets are statistically independent.

Since the slow decrease in $\Delta_2 E(N)$ is a classical effect—the increasing capacitance as the dot becomes bigger—we remove it by fitting a polynomial. To compare with experiments, the addition energy is scaled by the mean-level spacing found from the average electron density n through $\Delta = 2\pi\hbar^2\langle n \rangle / m^* N$; the resulting dimensionless spacing is denoted s [see Fig. 1(b)]. Note that the typical scale of s is 1; that is, fluctuations of the addition energy are on the scale of the single-particle mean-level spacing.

We find the distribution of s for even and odd N in three ranges of electron number, $N = 20\text{--}80$, $80\text{--}140$, and $140\text{--}200$, in both symmetric and asymmetric external potentials. (For the smallest, mean, and largest values of N , r_s is 2.5, 1.6, and 1.4, respectively.) The main features of the results, shown in Fig. 2, are as follows. (i) *Even/odd*: There is a difference in the distribution for N even or odd in the small N range, and the parity effect in the symmetric case is more pronounced than for asymmetric potentials. But there is a striking *absence* of even/odd effect in the asymmetric large N case [panel 2(f)]. (ii) *Shape*: The distributions are Gaussian-like. This extends the previous small N results, disagrees with the RPA-RMT results for large N , and is consistent with experiments [23,25] (where, however, the ground-state properties are obscured by temperature effects [14,15]). (iii) *Small/large*: The spacing distributions for small N are different from those for large N . Since the experimental QDs generally involve tens to hundreds of electrons, one must be cautious in generalizing to large dots conclusions drawn from studying small dots. (iv) *Symmetric/Asymmetric*: Both the variance of the peak spacing and the magnitude of the even/odd effect is larger in the symmetric case.

The insets in Fig. 2 show histograms of the spin distribution. A remarkable feature is the significantly *higher* fraction of high-spin ground states that we find at large N than in either previous SDFT investigations of small disordered dots [11] (for small N , we agree, of course, with previous results) or other investigations. Especially in the asymmetric case, $P(S = 1)$ is even higher than

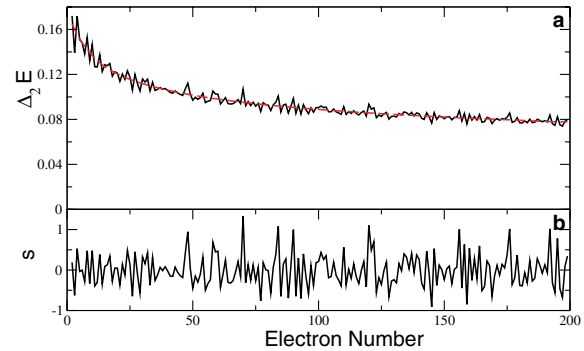


FIG. 1 (color online). Addition energy as a function of electron number. (a) Raw addition energy data (solid) and its polynomial fit (dashed) to remove the change in classical charging energy. (b) Addition energies scaled by the mean level spacing after removing smooth part ($\lambda = 0.6$ and $\gamma = 0$).

$P(S = 0)$ for $N = 80\text{--}200$. Again we see a clear dependence on the electron number range: while the spin distribution for odd N changes little as N increases, the spin distribution for even N is quite different for small and large N . Comparing spin distributions in the presence and absence of symmetry, we see a larger high-spin fraction in the asymmetric case for all three ranges of N .

This last result is at first surprising: generally one expects increased symmetry to increase the spin—as in

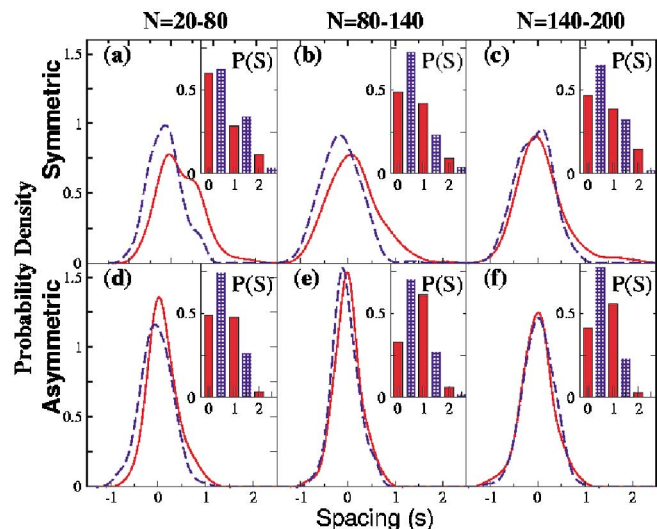


FIG. 2 (color online). Distributions of peak spacing, s , for even (solid) and odd (dashed) N . The columns correspond to the different ranges of electron number indicated, while the first row [(a)–(c)] is for a symmetric external potential and the second for asymmetric [(d)–(f)]. The inset of each figure shows the corresponding spin distribution for N even (solid) and odd (shaded). Both the lack of even/odd effect and the large spin in panel (f) is striking and indicates an unexpectedly large effective electron-electron interaction. (A sliding window is used in estimating the probability density, yielding a smooth curve rather than a histogram; each curve is made from 150 data points using a Gaussian window of width 0.3.)

Hund's rule for the spin of atoms. We can use random matrix theory, however, to show that there are competing effects here—the statistics of the eigenenergies vs the statistics of the eigenfunctions. For simplicity we consider the simplest RMT: a two-electron two-level model with no spatial correlations beyond a wavelength. In Hartree-Fock with the assumption that the orbitals remain the same for different spin configurations, the energy difference between the $S = 0$ and $S = 1$ states is

$$\delta E \equiv E_{S=1} - E_{S=0} = \delta \varepsilon + (J_{12} - K_{12}) - J_{11}, \quad (2)$$

where $\delta \varepsilon$ is the single-particle level spacing, $J_{ij} = \int d\mathbf{r}d\mathbf{r}' |\psi_i(\mathbf{r})|^2 v_{\text{scr}}(\mathbf{r}, \mathbf{r}') |\psi_j(\mathbf{r}')|^2$ are the Coulomb energies, and $K_{12} = \int d\mathbf{r}d\mathbf{r}' \psi_1^*(\mathbf{r}) \psi_2^*(\mathbf{r}') v_{\text{scr}}(\mathbf{r}, \mathbf{r}') \psi_1(\mathbf{r}') \psi_2(\mathbf{r})$ is the exchange energy. Here we use the screened potential $v_{\text{scr}}(\mathbf{r}, \mathbf{r}')$ in order to implicitly account for the other electrons. Qualitatively, the screened interaction is approximately zero range, $v_{\text{scr}}(\mathbf{r}, \mathbf{r}') \rightarrow (A\Delta/2)\delta(\mathbf{r} - \mathbf{r}')$ where Δ is the mean single-particle level spacing and A is the area. In this limit, the second term in Eq. (3) vanishes, and the third term is proportional to the “inverse participation ratio” (IPR) defined by $I \equiv A \int d\mathbf{r} |\psi(\mathbf{r})|^4$. Therefore, in the zero-range limit and considering the time reversibility of the system [33], we have

$$\delta E_{\text{zero-range}} = \delta \varepsilon - I\Delta/3. \quad (3)$$

There is clearly a competition here between the level spacing—a large spacing tends to decrease the spin—and the statistics of the wave functions—increased localization increases I and leads to a larger spin.

To see the competition explicitly, we calculate the distribution of the SPLS $\delta \varepsilon$ and that of the IPR from top-level KS orbital energies and wave functions in both the symmetric and asymmetric cases (see Fig. 3). While the symmetric case has a higher probability of small level spacing, the mean IPR is also smaller. Our overall result—the decrease in probability of $S = 1$ upon introducing symmetry [Fig. 2(f)]—shows that the effect of wave function statistics is stronger in our system.

The trend here is captured by random matrix theory. For an asymmetric chaotic potential, the distribution of the SPLS is that of the Gaussian orthogonal ensemble (GOE). In the symmetric case, however, the SPLS statistics is the superposition of four GOE's [17], one for each symmetry class. Figure 3(c) shows these two distributions. Clearly, the superposition greatly reduces the nearest-neighbor level repulsion, which implies that spatial symmetry favors a high-spin ground state, in accordance with Hund's rule.

For the wave function statistics, RMT suggests that the single-particle wave functions of classically chaotic systems are described by M -dimensional random unit vectors [2,34]. The shape of the resulting distribution of IPR depends on M , as shown in Fig. 3(d) for $M = 20$ and 80. These values of M are chosen to correspond to the

number of independent orbital levels: approximately $N/2$ in the asymmetric case because of spin, and $N/8$ for the fourfold symmetric potential. Symmetry reduces the effective M and so reduces the IPR, acting against a high-spin ground state. Hence there is a competition between the SPLS and the IPR.

The results in Fig. 3 show, of course, that the distributions of both the SPLS and the IPR agree with RMT only qualitatively. In particular, the fluctuation of the IPR is much smaller for the KS wave functions than in RMT. We believe this is due to the neglect of spatial correlations in our very simple RMT.

In summary, by studying a model 2D quantum dot with up to $N = 200$ electrons, we have found new phenomena. Both the statistics of ground-state spin and the spacing between conductance peaks depend on the electron number, as well as on the spatial symmetry. The results for large electron number and asymmetric potential are surprising: the shape of the peak-spacing distribution is Gaussian-like, the even/odd effect vanishes, and there is a substantial fraction of large-spin ground states ($S \geq 1$). These effects imply a strong effective or residual electron-electron interaction.

This is remarkable in that conditions in our dots are not extreme: $r_s \sim 1.5$ corresponds to a moderate bare interaction strength, and the dimensionless conductance is large, $g \sim 4$, comparable to the value in experiments. To obtain the spin and peak-spacing distributions that we find here from the RPA-RMT model requires an effective exchange constant of $J_s \sim 0.6\Delta$, larger than the maximum value possible in RPA. The origin of this unexpectedly large residual interaction is not presently known.

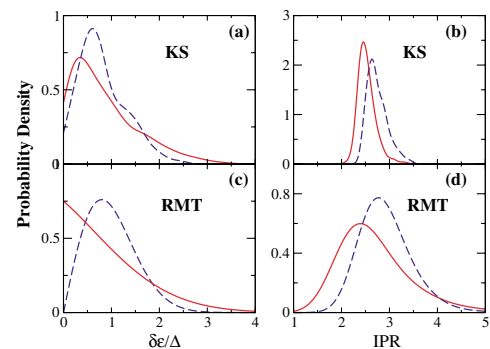


FIG. 3 (color online). Distributions of the single-particle level spacing (scaled by the mean) and the IPR from Kohn-Sham calculations and from random matrix theory. (a) The distribution of SPLS calculated from top KS orbital energies for symmetric (solid) and asymmetric (dashed) case, respectively. (b) The distribution of IPR calculated from top-level KS orbital wave functions for symmetric (solid) and asymmetric (dashed) case, respectively. (c) The distributions of SPLS for a single GOE (dashed) and the superposition of four GOE (solid) according to RMT. (d) The distributions of IPR calculated from the eigenvectors of real symmetric random matrix with dimension $M = 20$ (solid) and $M = 80$ (dashed).

We close with a caveat and a comment: First, this work is based on the 2D local spin density approximation whose validity, though already verified for *small* parabolic QD's [28,29], is not well tested for *large* nonparabolic quantum dots as studied here. Our result, though not definitive, highlights the need to go beyond RPA-RMT and perform a real Fermi liquid theory study. On the other hand, note the recent experimental work in Ref. [35] which, though still preliminary, indicates a high probability of large-spin ground states. The surprisingly large effective interactions found here suggest that more experiments should be a high priority.

We appreciate discussions with D. Ullmo and G. Usaj. This work was supported in part by NSF Grant No. DMR-0103003 and the North Carolina Supercomputing Center.

-
- [1] L. P. Kouwenhoven *et al.*, in *Mesoscopic Electron Transport*, edited by L. L. Sohn, G. Schön, and L. P. Kouwenhoven (Kluwer, Dordrecht, 1997), pp. 105–214.
- [2] Y. Alhassid, *Rev. Mod. Phys.* **72**, 895 (2000).
- [3] U. Sivan, R. Berkovits, Y. Aloni, O. Prus, A. Auerbach, and G. Ben-Yoseph, *Phys. Rev. Lett.* **77**, 1123 (1996).
- [4] R. Berkovits, *Phys. Rev. Lett.* **81**, 2128 (1998).
- [5] A. Cohen, K. Richter, and R. Berkovits, *Phys. Rev. B* **60**, 2536 (1999).
- [6] P. N. Walker, G. Montambaux, and Y. Gefen, *Phys. Rev. B* **60**, 2541 (1999).
- [7] S. Levit and D. Orgad, *Phys. Rev. B* **60**, 5549 (1999).
- [8] K. H. Ahn, K. Richter, and I. H. Lee, *Phys. Rev. Lett.* **83**, 4144 (1999).
- [9] L. Bonci and R. Berkovits, *Europhys. Lett.* **47**, 708 (1999).
- [10] M. Stopa, *Phys. Rev. B* **54**, 13767 (1996).
- [11] K. Hirose and N. S. Wingreen, *Phys. Rev. B* **65**, 193305 (2002).
- [12] Y. M. Blanter, A. D. Mirlin, and B. A. Muzykantskii, *Phys. Rev. Lett.* **78**, 2449 (1997).
- [13] D. Ullmo and H. U. Baranger, *Phys. Rev. B* **64**, 245324 (2001).
- [14] G. Usaj and H. U. Baranger, *Phys. Rev. B* **64**, 201319 (2001).
- [15] G. Usaj and H. U. Baranger, *Phys. Rev. B* **66**, 155333 (2002).
- [16] I. L. Aleiner, P. W. Brouwer, and L. I. Glazman, *Phys. Rep.* **358**, 309 (2002).
- [17] O. Bohigas, in *Chaos and Quantum Physics*, edited by M. J. Giannoni, A. Voros, and J. Jinn-Justin (North-Holland, Amsterdam, 1990), pp. 87–199.
- [18] P. W. Brouwer, Y. Oreg, and B. I. Halperin, *Phys. Rev. B* **60**, R13 977 (1999).
- [19] I. L. Kurland, I. L. Aleiner, and B. L. Altshuler, *Phys. Rev. B* **62**, 14 886 (2000).
- [20] P. Jacquod and A. D. Stone, *Phys. Rev. B* **64**, 214416 (2001).
- [21] Y. Oreg, P. W. Brouwer, X. Waintal, and B. I. Halperin, *cond-mat/0109541*.
- [22] F. Simmel, T. Heinzel, and D. A. Wharam, *Europhys. Lett.* **38**, 123 (1997).
- [23] S. R. Patel, S. M. Cronenwett, D. R. Stewart, A. G. Huibers, C. M. Marcus, C. I. Duruöz, J. S. Harris, K. Campman, and A. C. Gossard, *Phys. Rev. Lett.* **80**, 4522 (1998).
- [24] S. Lüscher, T. Heinzel, K. Ensslin, W. Wegscheider, and M. Bichler, *Phys. Rev. Lett.* **86**, 2118 (2001).
- [25] T. T. Ong, H. U. Baranger, D. M. Higdon, S. R. Patel, and C. M. Marcus (unpublished).
- [26] R. G. Parr and W. Yang, *Density-Functional Theory of Atoms and Molecules* (Oxford University Press, New York, 1989).
- [27] B. Tanatar and D. M. Ceperley, *Phys. Rev. B* **39**, 5005 (1989).
- [28] R. Egger, W. Häusler, C. H. Mak, and H. Grabert, *Phys. Rev. Lett.* **82**, 3320 (1999).
- [29] F. Pederiva, C. J. Umrigar, and E. Lipparini, *Phys. Rev. B* **62**, 8120 (2000).
- [30] We use a conjugated-gradient method to minimize the KS energy in the particle-in-box representation. The Hartree potential is calculated by a Fourier convolution approach. A simplified multigrid technique is used to accelerate the convergence.
- [31] O. Bohigas, S. Tomsovic, and D. Ullmo, *Phys. Rep.* **223**, 43 (1993).
- [32] The parameter values are as follows: In all cases, $a = 1.0 \times 10^{-4}$ and $b = \pi/4$. For the symmetric case $\gamma = 0$, we take λ to be 0.53, 0.6, 0.67, 0.74, and 0.81. For the asymmetric case we choose five sets of (λ, γ) : (0.53, 0.1), (0.565, 0.2), (0.6, 0.1), (0.635, 0.15), and (0.67, 0.1).
- [33] In the time-reversal symmetric case, there are three contributions to the average IPR, the direct, exchange, and Cooper pairings. However, when using the IPR to estimate interaction effects, higher-order processes in the screened interaction may renormalize the magnitude. This is well known for the Cooper channel—its final magnitude is small. We take this into account by using $2I/3$ in the estimate of the interaction effect.
- [34] N. Ullah, *Nucl. Phys.* **58**, 65 (1964).
- [35] J. A. Folk, C. M. Marcus, R. Berkovits, I. L. Kurland, I. L. Aleiner, and B. L. Altshuler, *Phys. Scr.* **T90**, 26 (2001).